PIBB 生物化学与生物物理进展
Progress in Biochemistry and Biophysics
2019,46(11):1101~1109
www.pibb.ac.cn

The Study on The Solution Structure of Full Length Primase From *Bacillus subtilis**

LUO Hao[1,2,3], LIU Wen-Lin[1,2,3], ZHOU Ying-Qin[1,2], TAO Mei[1,2,3], LIU Zhong-Chuan[1,2]**, WANG Gang-Gang[1,2]**

([1])*Key Laboratory of Environmental and Applied Microbiology, Chengdu Institute of Biology, Chinese Academy of Sciences, Chengdu* 610041, China;
[2])*Key Laboratory of Environmental Microbiology of Sichuan Province, Chengdu* 610041, China;
[3])*University of Chinese Academy of Sciences, Beijing* 100049, China)

Abstract In bacterial DNA replication, DnaG primase synthesizes RNA primers which are then extended by DNA polymerase. The DnaG primase consists of three domains, N-terminal zinc-binding domain (ZBD), RNA polymerase domain (RPD) and C-terminal helicase binding domain (HBD). In the process of producing primers, the three domains of primase cooperate with each other, and none is dispensable. Although the structures of the primase domains have been reported, so far, the full-length structure of the primase is not known yet. Here, the model of full-length DnaG in *Bacillus subtilis* (*Bsu*DnaG) was constructed from the data of X-ray small angle scattering (SAXS) analysis. The *Bsu*DnaG is in extended state in solution. On the other hand, the ZBD and HBD domains could exhibit continuous conformational changes relative to the RPD domain. This study suggests the domains rearrangement in DnaG primase may facilitate its function in DNA replication.

Key words DNA replication, primase, SAXS, flexibility
DOI: 10.16476/j.pibb.2019.0147

In DNA replication, the DNA polymerases are incapable of *de novo* synthesis, short oligonucleotides are produced by primase to support the initiation of nascent strands polymerization. In bacteria, DnaG primase uses the unwound single-stranded DNA as a template at the replication fork to synthesize RNA primers[1-2]. DnaG is composed of three domains, the N-terminal zinc-binding domain (ZBD), RNA polymerase domain (RPD) and C-terminal helicase binding domain (HBD). In DNA replication, the primase is recruited into the primosome by binding to hexameric DnaB helicase *via* HBD domain, then the ZBD/RPD recognizes the specific initiation site in the DNA template and the RPD synthesizes RNA primers. After priming, the primers are transferred to DNA polymerase for chain elongation. In this process, the primase communicates with DnaB helicase, DNA polymerase, single-strand DNA binding protein (SSB) and DNA template, which requests structural rearrangements of the primase domains[3-4]. Therefore, it is essential to study the full-length DnaG to understand how the DnaG domains cooperate with each other.

To date, the structures of primase domains in several bacteria have been resolved[5-12]. In *Aquifex aeolicus*, the crystal structure of ZBD/RPD revealed that ZBD docks against a face on the opposite side of the RPD from the active site. In *E. coli*, SAXS experiments show that the ZBD is bound to the RPD in compact mode, however, the *E. coli* ZBD/RPD fragment can transition to an extended state under condition of increased ionic strength[11]. So far, the structure of full-length primase is unknown, the

* This work was supported by grants from The National Natural Science Foundation of China (NSFC) (U1432102, 31700664, 31470742, 31700664, 31270783) and the 100 Talents Program of the Chinese Academy of Sciences.

** Corresponding author.
WANG Gang-Gang.
Tel: 86-28-82890828, E-mail: wanggg@cib.ac.cn
LIU Zhong-Chuan.
Tel: 86-28-82890823, E-mail: liuzhongch07@mails.ucas.ac.cn

Received: July 1, 2019 Accepted: October 14, 2019

flexibility of full-length DnaG has not been evaluated yet.

In this study, we purified the *Bacillus subtilis* DnaG (*Bsu*DnaG) and analyzed its solution structure by X-ray small angle scattering. For the first time, the rigid body model of the full-length DnaG primase was described, the *Bsu*DnaG primase was in extended state in solution. On the other hand, the flexibility analysis on *Bsu*DnaG indicated that the ZBD and HBD domains could exhibit continuous conformational changes relative to the RPD domain. These results show light on the mechanism how the *Bsu*DnaG function in DNA replication.

1 Materials and methods

1.1 Protein expression and purification

The expression and purification of *Bsu*DnaG were the same as previously described[8]. The purified protein was analyzed by SDS-PAGE and the purity of *Bsu*DnaG exceeded 95%. The protein was concentrated to ~15 g/L and stored at 4℃ for subsequent experiments.

1.2 Dynamic light-scattering (DLS) measurements

The particle size and uniformity of the *Bsu*DnaG protein were tested by the DynaPro NanoStar instrument (Wyatt, USA). The sample at a concentration of 5 g/L was added to the 10 μl quartz cuvette for measurement at 25℃, a total of ten scans of 5 s duration were accumulated. The light scattering data was analyzed to obtain the distribution of ion diffusion coefficient (*Dt*). For spherical particles, the diffusion constant can be interpreted as the hydrodynamic radius R_h of a diffusing sphere *via* the Stokes-Einstein equation $D_0 = k_B T/6\pi\eta R_h$ where k_B is the Boltzmann constant (1.381×10^{-23} J/K), T is the absolute temperature, and η is the viscosity of the solvent. Finally, the sizes distribution and the particle diameters distribution were estimated using the DYNAMICS software, which gave rise to an autocorrelation function.

1.3 Homology structural modeling

The 3D models of the ZBD and HBD of DnaG from *B. subtilis* were generated by SWISS-MODEL[13]. Structure validation and quality control were performed by Procheck[14]and WhatCheck[15] modules on the WhatIf server.

1.4 SAXS measurements and data processing

Experimental SAXS data were collected at the BL19U2 beamline at NCPSS (Shanghai, China)[16] on *Bsu*DnaG serially diluted to 1, 3, 5 and 7 g/L. Before SAXS measurements, all samples were centrifuged at 12 000 r/min for 10 min to remove aggregates and debris. Two millimolar DTT was added to samples to relieve radiation damage. Twenty successive frames were collected for each sample with the exposure time for each frame being 1 s. The scattering intensity $I(s)$ was recorded in the range of the momentum transfer, 0.02 Å < s < 0.4 Å, where $s = (4\pi\sin\theta)/\lambda$, 2θ is the scattering angle and λ = 1.54 Å. Owing to the high experimental noise for s values > 0.3 Å, the scattering data in the range of 0.02 to 0.3 Å was applied for structural analysis.

The composite scattering curve was generated from various protein sample concentrations by using ATSAS[17-18]and PRIMUS[19]. Data obtained from different sample concentrations were merged to yield the final composite scattering curve. The low resolution shape of *Bsu*DnaG was built by the *ab initio* method, DAMMIF[20]. Twenty models were compared and averaged by DAMAVER[21] and the most universal model was selected as the typical model. Currently, high-resolution crystal structures of ZBD and HBD of *Bsu*DnaG are not available. Thus, tertiary structure modeling was used to build atomistic representations of the *BsuDnaG* subdomains, then rigid body modeling was performed by using CORAL[17]. To evaluate the flexibility of *Bsu*DnaG, the enzyme with assemblies of different conformers was validated by using the ensemble optimization method (EOM)[22]. Standard parameters of EOM were used, which included the generation of 10 000 different structural conformations that were subjected to the selection of the ensemble distribution.

2 Results

2.1 Uniformity detection of *Bsu*DnaG protein

The *Bsu*DnaG protein was analyzed by SDS-PAGE (Figure 1a). The homogeneity of *Bsu*DnaG was evaluated by dynamic light scattering, as shown in Figure 1b, the light intensity autocorrelation function was smooth and continuous, exponentially decaying from a maximum value of 1.4 to a value of 1, illustrating that the *Bsu*DnaG protein was stable. Figure 1b illustrated that *Bsu*DnaG molecules were

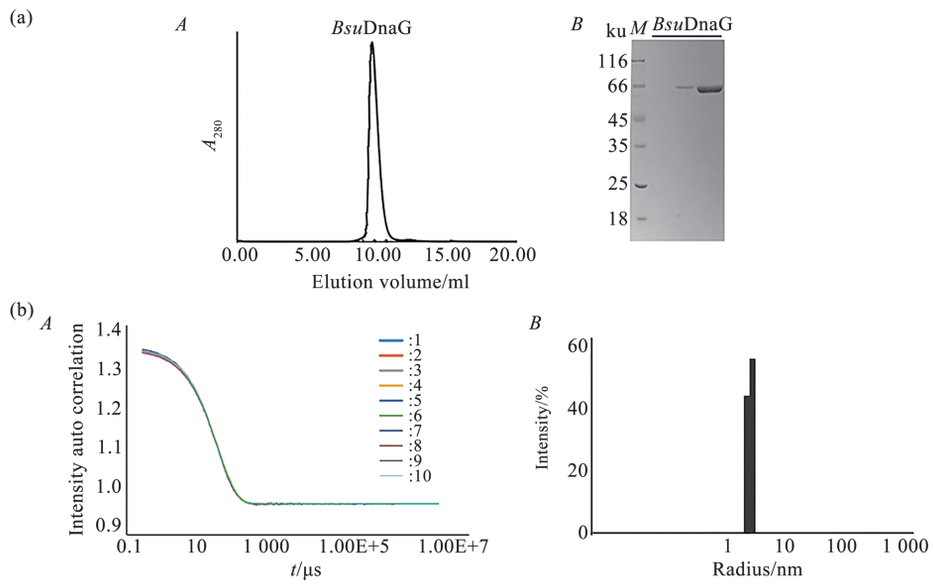

Fig. 1 The preparation of *Bsu*DnaG

(a) *A*: The gel filtration chromatogram of *Bsu*DnaG. The gel filtration column is Superdex 75 10/300 GL. *B*: The polyacrylamide gel electrophresis analysis on *Bsu*DnaG after gel filtration chromatogram. (b) *A*: The light intensity autocorrelation function of *Bsu*DnaG from dynamic light scattering analysis. The results of ten trials were marked with ten different colors, respectively. *B*: The size distribution of *Bsu*DnaG was shown in the regularization graph, which presented monomodal size distribution.

uniformly dispersed in the solution. Parameter statistics of *Bsu*DnaG was shown in Table 1. The measured molecular size of *Bsu*DnaG was about 4.3 nm and the predicted molecular mass was ~ 65 ku, which was close to the theoretical value of 69 ku, indicating that the protein was in a monomer state in solution.

Table 1 Parameter statistics of *Bsu*DnaG by DynaPro NanoStar

Item（*Bsu*DnaG）	Normalized intensity/(Cnt·s^{-1})	Radius/nm	Mw-S/ku
1	1793099	4.2	64.89
2	1798947	4.3	64.85
3	1820822	4.3	64.79
4	1816643	4.3	64.77
6	1844589	4.3	64.76
7	1783932	4.3	64.84
8	1770273	4.3	64.88
9	1800920	4.2	64.89
10	1787716	4.3	64.88

The numbers in the first column represent different tests.

2.2 The tertiary structure of ZBD and HBD of *Bsu*DnaG

The tertiary structures of ZBD and HBD of *Bsu*DnaG were modeled using SWISS-MODEL. The homology modeling of proteins by SWISS-MODEL requires a sequence consistency greater than 30%. Here, The *Bsu*DnaG ZBD (residues 1−97) shows 66% sequence identity to the ZBD of *Bst*DnaG (PDB ID: 1D0Q, chain A) [5], whereas the *Bsu*DnaG HBD (residues 462−602) has 51% sequence identity to the HBD of *Bst*DnaG (PDB ID: 2R6A, chain C) [12] (Figure 2a). The structures of ZBD and HBD from *Bst*DnaG are good template for homology modeling. The superposition of the models of ZBD and HBD from *Bsu*DnaG to the crystal structures of counterparts in *Bst*DnaG revealed a r.m.s.d value of 0.11 and 0.09 Å, respectively (Figure 2b). The geometry of the models was further validated by Procheck and WhatIf. The Ramachandran plots showed that 90.1 % of the amino acids in ZBD and 87.4 % in HBD fell in the preferred ϕ/ψ peptide torsion angle regions and none of the residues were in disallowed regions(Figure 2c). The overall geometry and packing validation parameters calculated by WhatIf also pointed to good-quality models. Therefore, the models of ZBD and HBD we obtained could be used to model the *Bsu*DnaG rigid body structure.

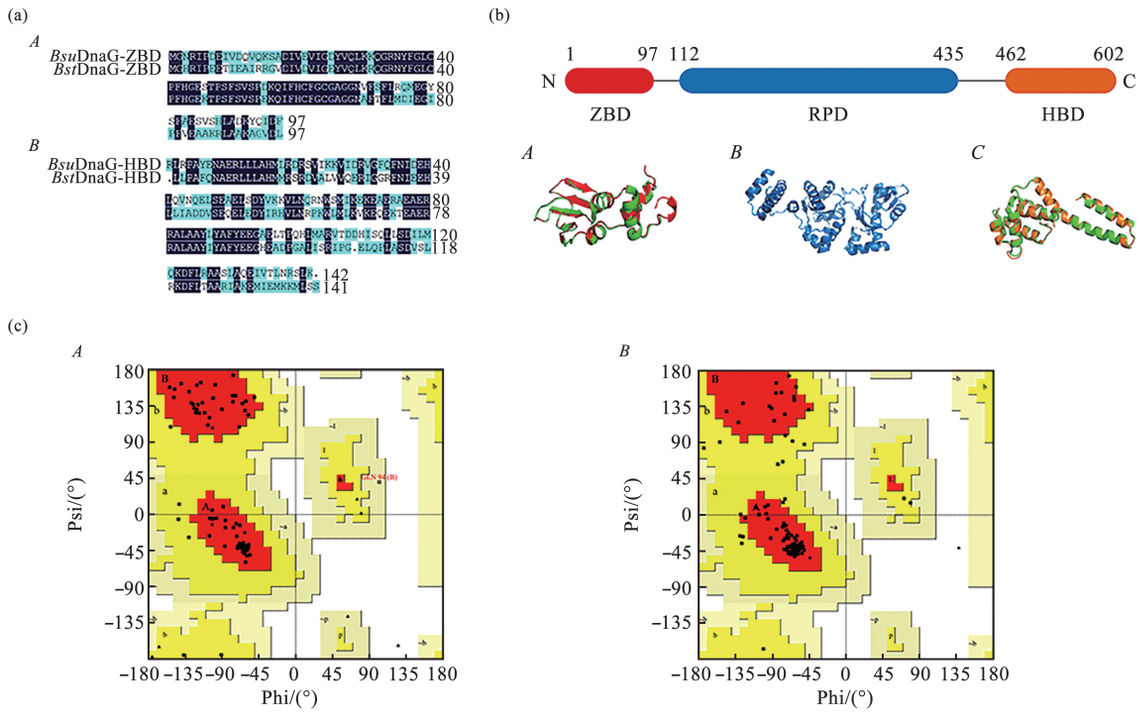

Fig. 2 The homology modeling of ZBD and HBD of *Bsu*DnaG

(a) *A*: Amino acid sequence alignment of *Bsu*DnaG and *Bst*DnaG Zinc binding domain (ZBD). *B*: Helicase binding domain (HBD). (b) The superposition of the models of ZBD and HBD in *B. subtilis* and the crystal structures of counterparts in *B. stearothermophilus*. The *Bsu*DnaG(ZBD), *Bsu*DnaG(RPD) and *Bsu*DnaG(HBD) domains were colored in red, blue and orange, and the *Bst*DnaG(ZBD) and *Bst*DnaG(HBD) were colored in green. (c) The Ramachandran plots of the constructed models of ZBD and HBD in *B. subtilis*. *A*: *Bsu*DnaG(ZBD). *B*: *Bsu*DnaG (HBD). The most favorite regions, the additional allowed regions, the generously allowed regions and the disallowed regions were colored in red, yellow, pink and white, respectively.

2.3 Solution structure of full−length *Bsu*DnaG

The SAXS profiles recorded of the *Bsu*DnaG are shown in Figure 3a. The radius of gyration (R_g) was ~ (37.3 ± 0.19) Å, which was evaluated to be within the range of the Guinier approximation. The molecular mass of *Bsu*DnaG was calculated to be (70 ± 2) ku, which is in agreement with the theoretical mass of 69 ku, indicating that the protein behaves as a monomer in solution. The distance distribution function *p(r)* for *Bsu*DnaG is shown in Figure 3b. Profiles of the *p(r)* function for *Bsu*DnaG in solution were characterized as an elongated body with a maximal particle dimension, D_{max}, of ~145 Å. In addition, twenty independent models were generated by *ab initio* modeling, which gave reproducible results and showed good approximations to the experimental data with a discrepancy value χ^2 = 1.17 (Figure 3a, green line). A specific model of *Bsu*DnaG was built by CORAL modeling using the structures of ZBD, RPD and HBD of *Bsu*DnaG as rigid bodies. The rigid model of CORAL (Figure 3c) agreed with the experimental data very well (χ^2 = 0.95) (Figure 3a, blue line). The model revealed that the HBD extends away from the other two domains (ZBD and RPD). Moreover, the CORAL reconstructions fitted to the DAMMIF models, as demonstrated in Figure 3d. Thus, these two independent methods are consistent, thereby supporting the notion that the models presented here clearly represent solution structures.

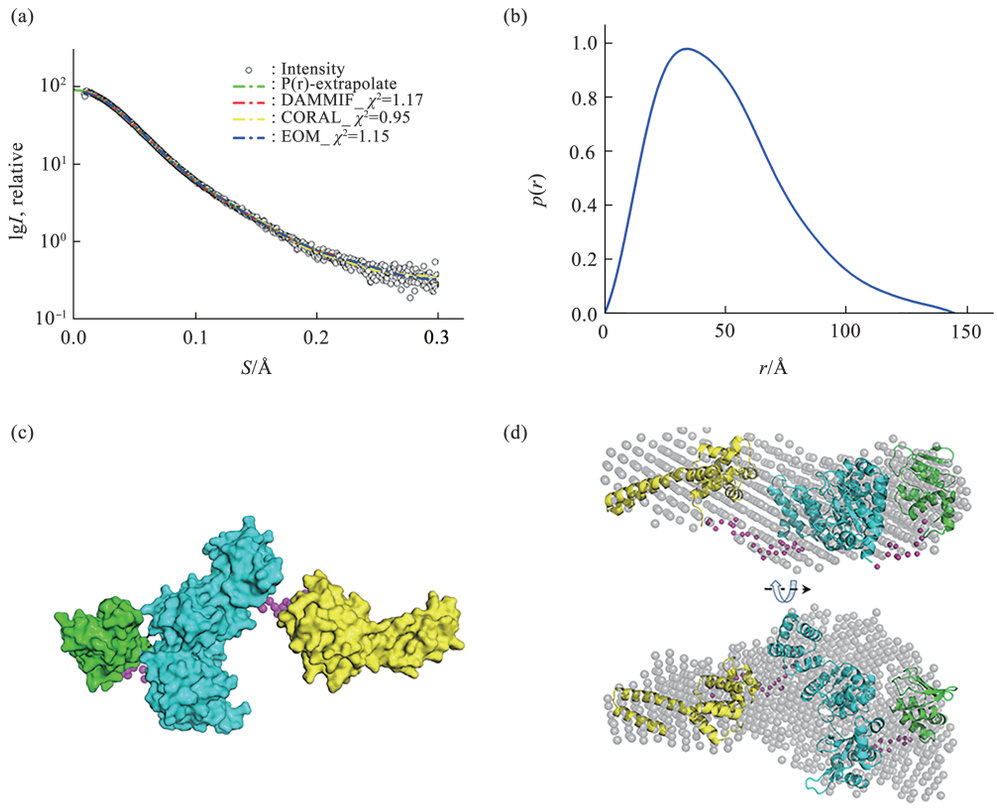

Fig. 3 Rigid body modeling of *Bsu*DnaG

(a) SAXS scattering profiles and model reconstructions of *Bsu*DnaG. Black circle: experimental intensity; green line: smooth curve back transformed from the $p(r)$ and extrapolated to zero scattering angle; red line: scattering pattern calculated from the DAMMIF model; yellow line:scattering pattern computed from CORAL model; blue line: averaged scattering pattern of the optimized models generated by EOM. (b) Distance distribution function $p(r)$ for full length *Bsu*DnaG in solution. (c) The rigid body modeling of full-length *Bsu*DnaG by CORAL, the ZBD, RPD and HBD domains were colored in green, blue and yellow, respectively. (d) Superposition of DAMMIF and CORAL models. The missing loops are represented as dummy residues colored purple. Two orientations were shown. The ZBD, RPD and HBD domains were colored in green, blue and yellow, respectively.

Given the intrinsic flexibility of *Bsu*DnaG, a large pool of 10 000 different conformations was generated by EOM and an optimized ensemble of 50 models that good described the SAXS data was selected. The selected ensemble of conformations is in good agreement with the SAXS profile with a χ^2 value of 1.15. Both the R_g and D_{max} distribution functions of the ensemble selected from the random pool for *Bsu*DnaG had a broad peak, ranging from ~25 to 50 Å and ~80 to 160 Å, respectively (Figure 4a, b). From the distributions of the optimized ensembles, the fractions of models with *Rg* ranging from 25.0 to 37.4 Å correspond to compact configuration, one representative model (*A*) from this *Rg* region was showed in Figure 4c, where the HBD bended at a large angle to approach the RPD domain. The other fractions of models (*Rg* between 37.5 and 50.0 Å) are rather extended, five representative models (*B*—*F*) from this *Rg* region were presented in Figure 4c. The parameters of the selected models were presented in Table 2. The histogram of the *Rg* distribution in Figure 4 resulted in an estimated value of ~50% for each type of the models. Although the conformations of *Bsu*DnaG were divided into two types according to flexibility analysis, even the compact conformations were looser than the folded globular proteins. These results suggested that full-length *Bsu*DnaG had a high degree of flexibility and underwent continuous conformational changes in solution, which may have an compact on the function of *Bsu*DnaG.

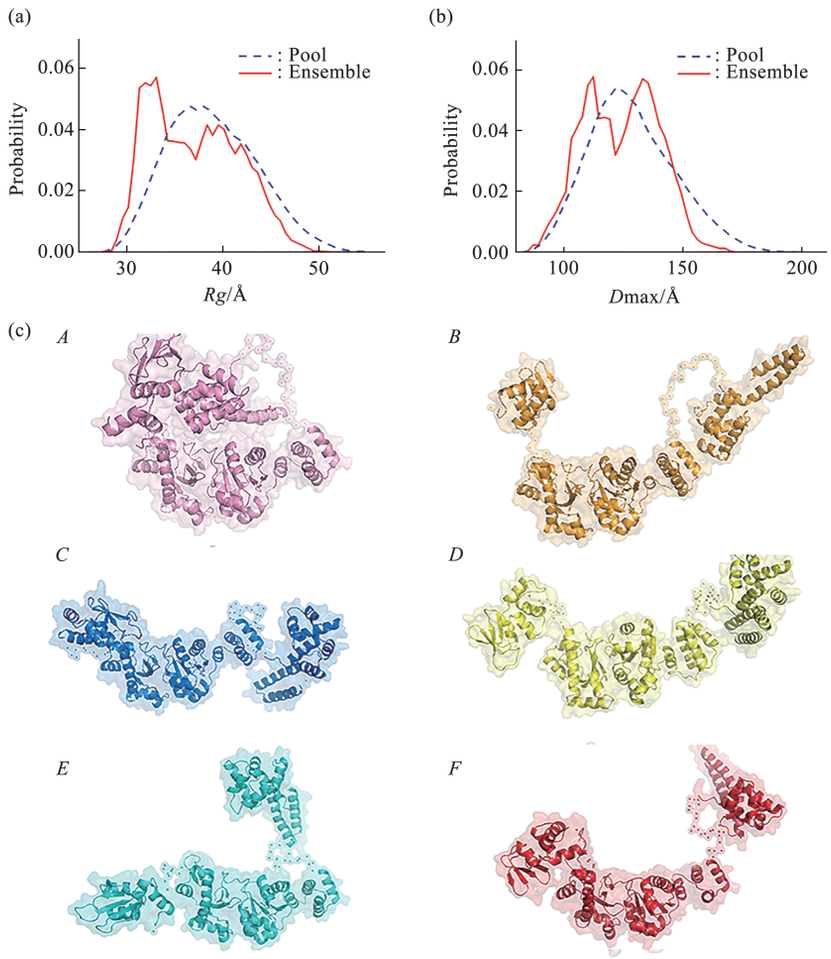

Fig. 4 Flexibility analysis of *Bsu*DnaG

(a, b) *Rg* and D_{max} distributions of the optimized ensembles for *Bsu*DnaG analyzed by program EOM, the χ^2 value was 1.15. (c) The optimal six *Bsu*DnaG solution models selected by EOM, labeled in six different colors, respectively.

Table 2 The parameters of the models selected by EOM program

Item	*Rg*/Å	*D*max/Å	Fraction
*Bsu*DnaG (*A*)	32.84	109.33	0.505
*Bsu*DnaG (*B*)	42.93	144.56	0.101
*Bsu*DnaG (*C*)	42.40	136.85	0.101
*Bsu*DnaG (*D*)	42.44	131.22	0.101
*Bsu*DnaG (*E*)	42.69	143.87	0.101
*Bsu*DnaG (*F*)	42.73	149.62	0.101

The letters in parentheses represent representative models selected by EOM program. Fraction represents the proportion of the representative model in all selected models.

3 Discussion

In bacteriophage T7, the primase is covalently linked to the helicase as a bifunctional protein; and hence, the primase stacks on the helicase ring at the DNA replication fork[23]. In humans, the primase heterodimer contains a small catalytic subunit (p49) and a large regulatory subunit (p58) with p49 responsible for primer synthesis and p58 responsible for template-primer binding. An 18-residue linker between the C-terminal domain of p58 (p58C) and the rest of the primase facilitates the movement of p58C during primer elongation[24-25]. For bacterial DnaG primase, the HBD tethers the DnaG with DnaB at the DNA replication fork and the ZBD/RPD is responsible for template binding and primer elongation. The intrinsic flexibility of DnaG results in the degradation of the protein *in vitro*, which has hampered the determination of the full-length

structure of *Bsu*DnaG[6,8]. Here, the rigid body model of *Bsu*DnaG obtained by CORAL (Figure 3c) showed that *Bsu*DnaG was stretched in solution, the HBD domain was far from the other two domains, the ZBD docked against the RPD and associated closely.

In DNA replication, the primase is recruited to the DNA replication fork by binding to the helicase across the HBD[12,26-27]. After priming, the polymerase competes with primase to interact with SSB for the primer hand-off to DNA polymerase[28]. Otherwise, the C-terminal domain of DnaG is also responsible for binding to the SSB[29]. In these unwinding-priming-polymerizing processes, the primase communicates with both DNA and other proteins in the replisome, structural rearrangement is not dispensable. In primase, the flexibility of the interdomain linkers provides significant conformational freedom. Sequence alignment reveals that the RPD and HBD domains are connected by long loop region (Loop2), however, the length of the hinge region between ZBD and RPD domains (Loop1) is different (Figure 5). In *A. aeolicus* primase, Loop1 is eight residues shorter than that of *Bsu*DnaG, which may limit the rearrangement of ZBD domain. We analyzed the flexibility of *Bsu*DnaG through EOM, the results showed that *Bsu*DnaG underwent continuous conformational changes in solution (Figure 4), the ZBD domain and HBD domain could be rearranged at various angles relative to the RPD domain (Figure 4c) in each model, which implied that the *Bsu*DnaG could adapt to specific conformation upon interacting with each partner. To validate how DnaG interacts with partners in DNA replication initiation, further investigations on the structure of DnaG/partner complex are requested.

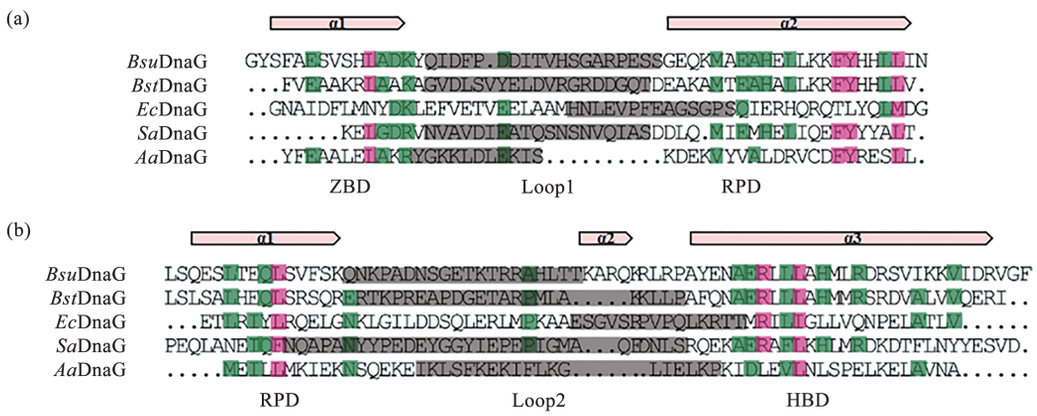

Fig. 5 Sequence alignments of the hinge regions between *Bsu*DnaG domains

(a) Loop1 between ZBD and RPD domains in five bacterial primases. *Bsu*DnaG: *Bacillus subtilis*; *Bst*DnaG: *Bacillus stearothermophilus*; *Ec*DnaG:*Escherichia coli*; *Sa*DnaG: *Staphylococcus aureus*; *Aa*DnaG: *Aquifex aeolicus*. (b) Loop2 between between RPD and HBD domains. Amino acid conservation among bacterial primases is mapped as a continuum of pink (most conserved) to white (least conserved), and the hinge area is marked in gray. The secondary structures of *Bsu*DnaG fragments were predicted by PSIPRED (http://bioinf.cs.ucl.ac.uk/psipred/).

Acknowledgments The staff at beamline BL19U2 of the Shanghai Synchrotron Radiation Facilities are gratefully acknowledged for efficient support.

References

[1] Chodavarapu S, Kaguni J M. Replication initiation in bacteria. Enzymes, 2016, **39**: 1-30

[2] Mott M L, Berger J M. DNA replication initiation: mechanisms and regulation in bacteria. Nat Rev Microbiol, 2007, **5**(5): 343-354

[3] Rodina A, Godson G N. Role of conserved amino acids in the catalytic activity of *Escherichia coli* primase. J Bacteriol, 2006, **188**(10): 3614-3621

[4] Corn J E, Pelton J G, Berger J M. Identification of a DNA primase template tracking site redefines the geometry of primer synthesis. Nature Structural & Molecular Biology, 2008, **15**(2): 163-169

[5] Pan H, Wigley D B. Structure of the zinc-binding domain of *Bacillus stearothermophilus* DNA primase. Structure, 2000, **8**(3): 231-239

[6] Kusakabe T, Richardson C C. The role of the zinc motif in sequence recognition by DNA primases. J Biol Chem, 1996, **271**(32): 19563-19570

[7] Keck J L, Roche D D, Lynch A S, *et al*. Structure of the RNA polymerase domain of *E. coli* primase. Science, 2000, **287**(5462): 2482-2486

[8] Zhou Y, Luo H, Liu Z, *et al*. Structural insight into the specific DNA template binding to DnaG primase in bacteria. Scientific Reports, 2017, **7**(1): 659

[9] Oakley A J, Loscha K V, Schaeffer P M, *et al*. Crystal and solution structures of the helicase-binding domain of *Escherichia coli* primase. J Biol Chem, 2005, **280**(12): 11495-11504

[10] Su X C, Schaeffer P M, Loscha K V, *et al*. Monomeric solution structure of the helicase-binding domain of *Escherichia coli* DnaG primase. The FEBS Journal, 2006, **273**(21): 4997-5009

[11] Corn J E, Pease P J, Hura G L, *et al*. Crosstalk between primase subunits can act to regulate primer synthesis in trans. Molecular Cell, 2005, **20**(3): 391-401

[12] Bailey S, Eliason W K, Steitz T A. Structure of hexameric DnaB helicase and its complex with a domain of DnaG primase. Science, 2007, **318**(5849): 459-463

[13] Biasini M, Bienert S, Waterhouse A, *et al*. SWISS-MODEL: modelling protein tertiary and quaternary structure using evolutionary information. Nucleic Acids Res, 2014, **42**(Web Server issue):252-258

[14] Laskowski R A, Macarthur M W, Moss D S, *et al*. PROCHECK: a program to check the stereochemical quality of protein structures. Journal of Applied Crystallography, 1993, **26**(2): 283-291

[15] Vriend G. WHAT IF: a molecular modeling and drug design program. Journal of Molecular Graphics, 1990, **8**(1):52-56

[16] Li N, Li X, Wang Y, *et al*. The new NCPSS BL19U2 beamline at the SSRF for small-angle X-ray scattering from biological macromolecules in solution. Journal of Applied Crystallography, 2016, **49**(5): 1428-1432

[17] Petoukhov M V, Franke D, Shkumatov A V, *et al*. New developments in the ATSAS program package for small-angle scattering data analysis. J Appl Crystallogr, 2012, **45**(2): 342-350

[18] Franke D, Petoukhov M V, Konarev P V, *et al*. ATSAS 2.8: a comprehensive data analysis suite for small-angle scattering from macromolecular solutions. J Appl Crystallogr, 2017, **50**(4): 1212-1225

[19] Konarev P V, Volkov V V, Sokolova A V, *et al*. PRIMUS: a Windows PC-based system for small-angle scattering data analysis. Journal of Applied Crystallography, 2003, **36**(5): 1277-1282

[20] Franke D, Svergun D I. DAMMIF, a program for rapid ab-initio shape determination in small-angle scattering. J Appl Crystallogr, 2009, **42**(2): 342-346

[21] Volkov V V, Svergun D I. Uniqueness of ab initio shape determination in small-angle scattering. Journal of Applied Crystallography, 2003, **36**(3): 860-864

[22] Tria G, Mertens H D, Kachala M, *et al*. Advanced ensemble modelling of flexible macromolecules using X-ray solution scattering. IUCrJ, 2015, **2**(2): 207-217

[23] Arkadiusz W, Kulczyk A M, Meyer P, *et al*. Cryo-EM structure of the replisome reveals multiple interactions coordinating DNA synthesis. PNAS, 2017, **114**(10): 1848-1856

[24] Baranovskiy A G, Zhang Y, Suwa Y, *et al*. Insight into the human DNA primase Interaction with template-primer. J Biol Chem, 2016, **291**(9): 4793-4802

[25] Baranovskiy A G, Zhang Y, Suwa Y, *et al*. Crystal structure of the human primase. J Biol Chem, 2015, **290**(9): 5635-5646

[26] Yang M, Wang G. ATPase activity measurement of DNA replicative helicase from *Bacillus stearothermophilus* by malachite green method. Analytical Biochemistry, 2016, **509**: 46-49

[27] Chintakayala K, Larson M A, Grainger W H, *et al*. Domain swapping reveals that the C- and N-terminal domains of DnaG and DnaB, respectively, are functional homologues. Molecular Microbiology, 2007, **63**(6): 1629-1639

[28] Yuzhakov A, Kelman Z, O'donnell M. Trading places on DNA-a three-point switch underlies primer hand off from primase to the replicative DNA polymerase. Cell, 1999, **96**(1): 153-163

[29] Naue N, Beerbaum M, Bogutzki A, *et al*. The helicase-binding domain of *Escherichia coli* DnaG primase interacts with the highly conserved C-terminal region of single-stranded DNA-binding protein. Nucleic Acids Res, 2013, **41**(8): 4507-4517

枯草芽孢杆菌全长引物酶的溶液结构研究*

罗　昊[1,2,3)]　刘文林[1,2,3)]　周迎芹[1,2)]　陶　美[1,2,3)]　刘忠川[1,2)**]　王刚刚[1,2)**]

([1)] 中国科学院应用与环境微生物重点实验室，成都 610041；

[2)] 环境微生物四川省重点实验室，成都 610041；

[3)] 中国科学院大学，北京 100049）

摘要　在细菌DNA复制中，DnaG引物酶合成RNA引物，然后合成的引物通过DNA聚合酶进行延伸. DnaG引物酶由3个结构域组成，N端锌结合结构域（zinc-binding domain，ZBD）、RNA聚合酶结构域（RNA polymerase domain，RPD）和C端解旋酶结合结构域（helicase binding domain，HBD）. 在合成引物的过程中，引物酶的3个结构域协同作用，缺一不可. 尽管引物酶3个结构域的结构均已有研究报道，但到目前为止，引物酶的全长结构尚不清楚. 我们在上海光源利用小角X射线散射技术研究了枯草芽孢杆菌全长引物酶的溶液结构，首次构建了全长引物酶结构模型. 我们发现，枯草芽孢杆菌引物酶在溶液中处于伸展状态，且ZBD和HBD结构域相对于RPD结构域呈现出连续的构象变化. 本文研究表明DnaG引物酶中的结构域重排可能有助于其在DNA复制中发挥功能.

关键词　DNA复制体，引物酶，小角X射线散射，柔性

中图分类号　Q71，Q937　　**DOI**：10.16476/j.pibb.2019.0147

* 国家自然科学基金（U1432102，31700664，31470742，31700664，31270783）和中国科学院百人计划资助项目.

** 通讯联系人.

王刚刚. Tel：028-82890828；E-mail：wanggg@cib.ac.cn

刘忠川. Tel：028-82890823；E-mail：liuzhongch07@mails.ucas.ac.cn

收稿日期：2019-07-01，接受日期：2019-10-14